Journal of Alloys and Compounds, 207/208 (1994) 192–195
JALCOM 3033

On the rare-earth cyanides $Ln[T(CN)_6]_{3/4} \cdot nH_2O$ (T=Fe, Ru)

F. Hulliger and H. Vetsch
Laboratorium für Festkörperphysik, ETH Hönggerberg, CH-8093 Zürich (Switzerland)

V. Gramlich
Institut für Kristallographie, ETH Zentrum, CH-8092 Zürich (Switzerland)

Xiao-Lin Xu
Institut für Anorganische Chemie der Universität, CH-8057 Zürich (Switzerland)

Abstract

With Ln=La, Ce, Pr, Nd, the title compounds crystallize in a defective derivative of the hexagonal $LaFe(CN)_6 \cdot 5H_2O$ structure where additional H_2O is replacing one quarter of $[Fe(CN)_6]^{3-}$. With the heavier Ln elements, we obtained orthorhombic (Fe) or monoclinic (Ru) and hexagonal (Fe, Ru) phases which appear to differ from the archetype only in details. Thermal dehydration destroyed the crystalline order almost completely and above 300 °C the cyanides decompose irreversibly.

1. Introduction

Among the rare earth (Ln) transition-element (T) cyanides, a valence transition from T^{III} to T^{II} is possible within virtually the same structure by the substitution $T^{III}(H_2O) \rightarrow T^{II}M^+$. Quite a number of corresponding pairs $Ln^{3+}T^{III}(CN)_6 \cdot nH_2O \leftrightarrow M^+Ln^{3+}T^{II}(CN)_6 \cdot (n-1)H_2O$ have been characterized in recent years [1–9]. The compounds with the larger Ln atoms crystallize in a hexagonal structure with $n=5$, whereas with the smaller Ln atoms (where $n=4$), an orthorhombic structure (a distorted defective derivative of the hexagonal archetype) is adopted.

We wondered whether this simple mechanism is restricted to the monovalent cations K^+, Rb^+, Cs^+, NH_4^+, Tl^+, or could also be applied to higher-valent cations. With divalent and trivalent cations, the analogous substitutions would be $T^{III}(H_2O)_{1/2} \rightarrow T^{II}(M^{2+})_{1/2}$ and $T^{III}(H_2O)_{1/3} \rightarrow T^{II}(M^{3+})_{1/3}$, respectively. We did not find any examples in the literature for the former case but there is no scarcity of examples for the latter case. Thus, Kuznetsov *et al.* [10] reported on the preparation of $Ce_4[Fe(CN)_6]_3 \cdot 14H_2O$ and Kuznetsov and Yakovleva [11] summarized the results on $Pr_4[Fe(CN)_6]_3 \cdot 10H_2O$, $Nd_4[Fe(CN)_6]_3 \cdot 10H_2O$, $Sm_4[Fe(CN)_6]_3 \cdot 10H_2O$, $Gd_4[Fe(CN)_6]_3 \cdot 14H_2O$, $Er_4[Fe(CN)_6]_3 \cdot 16H_2O$, $Yb_4[Fe(CN)_6]_3 \cdot 10H_2O$. The water content given for the cerium compound appeared to support our expectation, whereas that of the erbium compound rather should have been 11 instead of the reported $16H_2O$. These water contents all were based on chemical analyses. The water content derived from TGA measurements by Kralik *et al.* [12] for $Pr_4[Ru(CN)_6]_3 \cdot xH_2O$, $x=25$ and 30, however, showed that we had to be prepared for a surprise.

2. Experimental details

Crystalline powders of both the Fe and the Ru series were obtained according to the following reaction in neutral or slightly acidified aqueous solution:

$$4LnCl_3 + 3Li_4[T(CN)_6] \longrightarrow Ln_4[T(CN)_6]_3 \cdot xH_2O + 12LiCl$$

As a typical example, we describe the preparation of $Sm_4[Ru(CN)_6]_3 \cdot 26H_2O$. Commercial $K_4Ru(CN)_6] \cdot 3H_2O$ (p.A., Merck) was carefully transformed by the ether method [13] with LiOH to K-free $Li_4Ru(CN)_6$ [14]. Following Kralik *et al.* [12], we mixed the two solutions, 4 ml of 1 M $SmCl_3$ + 25 ml of H_2O dist. and 6 ml of 0.5 M $Li_4Ru(CN)_6$ + 25 ml of H_2O dist. The microcrystals were collected by filtering the solution after 1 h. The Sm content was determined with the titration method of Patton and Reeder [15], 32.0 wt.% in our example. For the determination of the $[Ru(CN)_6]$

SSDI 0925-8388(93)03033-F

TABLE 1. Crystallographic data for the cyanides $Ln[Fe(CN)_6]_{3/4}\cdot nH_2O$; $T=295$ K. The n values derived from the TGA measurements are rounded to 0.05; those marked with an asterisk refer to preparations from boiling neutral solutions. $\delta=10^3(a\sqrt{3}/b-1)$ is a measure for the orthorhombic deformation of the hexagonal archetype cell. Statistical standard deviations are added in parentheses. The effective error, however, may be at least twice as large

Ln	n	a (Å)	b (Å)	c (Å)	δ	V (Å^3)
La	6.1	7.3084(3)		14.0802(9)		651.3(1)
Ce	6.2	7.2881(3)		14.0415(10)		645.9(1)
Pr	6.2	7.2737(4)		14.003(2)		641.6(2)
Nd	5.9	7.2618(3)		13.9523(9)		637.18(9)
Sm	5.05	7.3120(4)		13.6985(12)		634.3(2)
	4.7*	7.3206(3)		13.6969(6)		635.70(8)
Eu	4.65	7.3405(23)	12.6746(15)	13.635(3)	+3.1(4)	1268.6(8)
	4.55	7.3215(4)		13.6278(8)		632.6(2)
	4.5*	7.3288(13)		13.607(2)		632.9(4)
Gd	5.05	7.3446(6)	12.6610(8)	13.6104(12)	+4.8(2)	1265.6(3)
Tb	4.65	7.3399(7)	12.6246(9)	13.562(2)	+7.0(2)	1256.7(4)
	4.75	7.2994(5)		13.5416(9)		624.9(2)
	4.35*	7.3104(8)		13.523(2)		625.9(3)
Dy	4.8	7.3327(3)	12.6012(4)	13.5194(6)	+7.9(1)	1249.2(2)
Ho	5.05	7.3255(5)	12.5840(6)	13.439(1)	+8.3(2)	1243.8(3)
Er	4.75	7.3200(3)	12.5688(5)	13.4537(8)	+8.74(8)	1237.8(2)
	4.95	7.2860(3)		13.4493(6)		618.3(1)
	5.2	7.2773(2)		13.4686(5)		617.7(1)
Tm	4.85	7.3114(5)	12.5447(8)	13.4142(9)	+9.5(2)	1230.3(2)
Yb	4.95	7.2599(2)		13.3364(5)		608.73(5)
	5.0	7.290(3)	12.550(4)	13.393(7)	+6.1(7)	1225.3(1.3)
Lu	4.65	7.3070(5)	12.5210(9)	13.3285(12)	+10.8(2)	1219.4(3)
	4.75	7.2556(3)		13.3194(6)		607.24(7)
	4.95*	7.2583(4)		13.3272(9)		608.05(11)
Y	5.1	7.3248(5)	12.5914(6)	13.5150(12)	+7.6(1)	1246.5(3)
	5.05	7.2917(7)		13.511(2)		622.1(2)

content, we transformed the compound into $Ag_4Ru(CN)_6$ and found 40.7 wt.%, which leads to a Sm to $[Ru(CN)_6]^{4-}$ ratio of 1:0.74. The water content was determined from thermogravimetric analyses (TGA) carried out up to 300–400 °C on a Mettler thermobalance. About 60 mg of cyanide powder contained in an alumina container were heated in flowing dry air at a heating rate of either 0.3 or 0.6 °C/min with Al_2O_3 powder as reference. The room-temperature lattice parameters were derived from Guinier patterns taken with Cu $K\alpha_1$ radiation and Si as internal standard (assuming $a=5.43047$ Å at 22 °C). Indexing was somewhat problematic in those cases where we obtained only mixtures of two modifications (*e.g.* with $Eu[Fe(CN)_6]_{3/4}\cdot nH_2O$), which is reflected in Tables 1 and 2 by the large errors. The thermal variation of the structure was investigated for three examples up to 270 °C with a Guinier–Lenné camera at a heating rate of 0.3 °C/min, *i.e.* virtually under the same conditions as the TGA measurements.

3. Results

The Guinier patterns of the cyanides with the large rare-earth elements La, Ce, ... were readily indexed in analogy to the hexagonal $KLaFe(CN)_6\cdot 4H_2O$ [2]. The unit cells, however, turned out to be definitely smaller than expected for the substitutional model. If for the hexagonal compounds, $M^+Ln^{III}T^{II}(CN)_6\cdot 4H_2O$ we plot $d=(V/Z)^{1/3}$ versus r_{M^+}, then the data point to a "cation" d-value for $Ln_{4/3}[T(CN)_6]\cdot 14/3H_2O$ about midway between K^+ and Na^+, 0.2–0.25 Å smaller than r_{K^+}, which is twice the difference we expected. This fact eliminated the simple model, at least for the hexagonal compounds. The possibility of including $(H_3O)^+$ as M^+ is excluded by the chemical analysis which confirmed the 4:3 ratio of Ln:Fe, Ru. An alternative model, still derived from the archetype structure, but warranting a smaller volume, obviously is the defect structure $Ln[T(CN)_6]_{3/4}\cdot[X]_{1/4}\cdot 5H_2O$, where X

TABLE 2. Crystallographic data for cyanides $Ln[Ru(CN)_6]_{3/4}\cdot nH_2O$; $T=295$ K. The n values derived from the TGA measurements are rounded to 0.05

Ln	n	a (Å)	b (Å)	c (Å)	β (°)	V (Å^3)
La	6.3	7.3844(2)		14.3645(6)		678.35(7)
Ce	6.5	7.3726(3)		14.3066(8)		673.46(8)
Pr	6.45	7.3594(2)		14.2977(5)		670.64(6)
Nd	6.45	7.3508(3)		14.2787(8)		668.18(8)
		7.3744(4)		14.3571(7)		676.17(9)
Sm	6.35	7.3833(7)	14.0979(14)	7.5784(6)	118.493(7)	693.3(3)
Eu	6.3	7.5646(9)	14.062(3)	7.3682(8)	118.440(9)	689.2(3)
Gd	6.35	7.5548(9)	14.031(2)	7.3525(7)	118.244(10)	686.0(3)
Tb	6.4	7.5231(7)	14.004(2)	7.3370(6)	118.398(7)	680.0(3)
Dy	6.3	7.504(4)	13.958(7)	7.332(3)	118.35(3)	675.9(9)
	6.1	7.5178(6)	13.9460(13)	7.3220(6)	118.312(7)	675.8(3)
	5.7	7.5186(6)	12.7607(9)	13.9810(7)		1341.4(3)
Ho	6.65	7.4961(7)	13.9434(12)	7.3155(8)	118.349(9)	672.9(3)
Er	6.45	7.483(4)	13.912(5)	7.320(4)	118.4(4)	670.2(1.1)
		7.438(7)		13.964(7)		668.9(6)
Tm	6.35	7.441(6)	13.905(13)	7.296(7)	118.37(8)	664(2)
		7.4105(6)		13.9128(12)		661.7(2)
Yb	6.25	7.437(2)	13.8404(23)	7.288(2)	118.42(2)	659.8(7)
		7.4038(3)		13.8658(7)		658.23(8)
Lu	6.15	7.441(4)	13.828(5)	7.266(4)	118.46(5)	657(2)
		7.3942(4)		13.8207(9)		654.4(1)
Y	6.5	7.4992(7)	13.9596(12)	7.3181(5)	118.313(7)	674.5(3)

may represent $(H_2O)_6$, $LiCl(H_2O)_4$, ... or, although rather improbable, just a vacancy. The first version was supported by the TGA measurements and finally confirmed by a structure determination on $La[Fe(CN)_6]_{3/4}\cdot 6.5H_2O$ and $La[Ru(CN)_6]_{3/4}\cdot 6.5H_2O$ although it is not completely safe to exclude the second version in the case of the Fe compound [17]. It is not surprising that partial ordering of the "holes" brings in an additional complication. Ordering and water content strongly depend on the synthesis conditions (temperature, concentration and acidity of the reactants, ...). The lattice parameters listed in Tables 1 and 2 therefore only describe the subcells.

In the heavy Ln series, acid solutions appear to favor the crystallization of the orthorhombic and monoclinic modifications, whereas in neutral solutions the hexagonal modifications formed. Figure 1 shows a plot of $d=(V/Z)^{1/3}$ versus $r_{Ln^{3+}}$. As in the alkali analogs, an abrupt change occurs between Nd and Sm, but in contrast to the alkali compounds, the cell volumes of the Fe salts increase although the water content decreases (for comparison we included the corresponding data for the $KLnFe(CN)_6\cdot nH_2O$ series). According to the TGA measurements, the water content n is 6–6.2 and 6.2–6.5 in the hexagonal Fe and Ru salts, respectively. It drops to about 5 in the orthorhombic Fe salts, but remains above 6 in the monoclinic Ru salts (the samples with the heavier Ln were always mixed with a hexagonal species of nearly the same unit-cell volume). Since in the Ru compounds, the water content is not reduced, the volume increase is much more pronounced here. The crystal structures of both the orthorhombic Fe salts (space group *Pbnm*?) as well as the monoclinic Ru salts (space group $P2_1/m$?) appear to be closely related to the hexagonal archetype but they may contain additional atoms. The $d=(V/Z)^{1/3}$ versus r_{M^+} plot for the Ru compounds leads to a hypothetical cation radius in the $KYFe(CN)_6\cdot 3H_2O$ model close to that of Rb^+ which is definitely larger than the average radius expected for $(Ln^{3+})_{1/3}(H_2O)_{2/3}$. It is noteworthy that the dependence of $\delta=10^3(a\sqrt{3}/b-1)$ on $r_{Ln^{3+}}$ is opposite to what is observed in the $M^+LnFe(CN)_6\cdot 3H_2O$ series which reflects the structural differences. Unfortunately, we have not been successful up to now in our attempts to grow crystals large enough for a single-crystal structure determination.

In the high-temperature behavior, the defect cyanides also differ distinctly from the alkali counterparts $M^+Ln^{II}(CN)_6\cdot nH_2O$. The sharp diffraction lines of

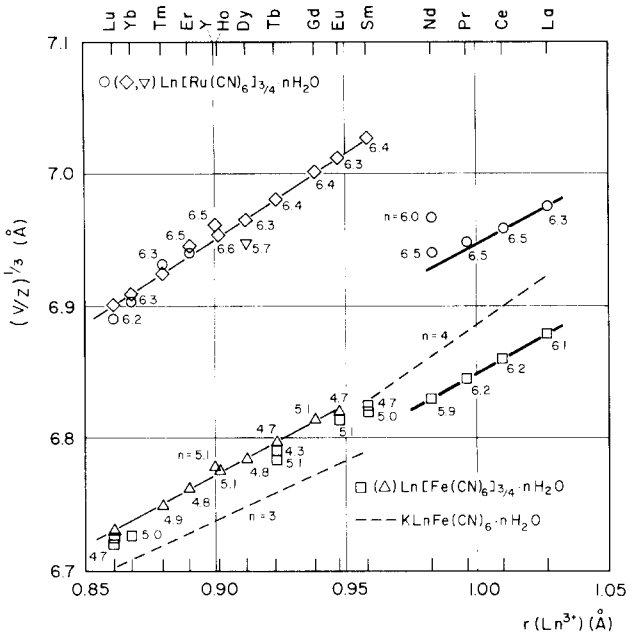

Fig. 1. The characteristic length $d=(V/Z)^{1/3}$ (where V/Z = unit-cell volume per formula unit of $Ln[Fe(CN)_6]_{3/4}\cdot nH_2O$ and $Ln[Ru(CN)_6]_{3/4}\cdot nH_2O$ is plotted versus the radius of the trivalent rare-earth ion [16]. The faint lines connect compounds the composition of which is not yet exactly established. The figures written near the symbols are the water content derived from TGA measurements. In the case of the heavy Ln compounds, they refer to a mixture of both modifications (which may slightly differ in composition). The broken lines represent the data for the $KLnFe(CN)_6\cdot nH_2O$ series for comparison.

$La[Fe(CN)_6]_{3/4}\cdot xH_2O$ and $La[Ru(CN)_6]_{3/4}\cdot xH_2O$ disappeared above 70 °C and 85 °C, respectively, and only the strongest low-angle lines (002, 101, 102), persisted up to 270 °C as extremely diffuse and broad shadows. In the orthorhombic $Tb[Fe(CN)_6]_{3/4}\cdot xH_2O$, the diffraction lines fade above 100 °C. The TGA curves are consistent with these findings. The weight loss on heating is very pronounced between 80 and 150 °C. Dehydration is terminated near 200 °C (190–230 °C) in the Fe salts, and between 240 and 270 °C in the Ru salts. The water-free cyanides are stable only in a rather small temperature range of 30–80 °C. Above 300 °C, they decompose, which is demonstrated by the fact that they can no longer be transformed back to the initial state by storing them in humid air, in contrast to the dehydrated cyanides.

Dehydration causes a distinct shrinking of the unit cell. While the c axis undergoes a rather abrupt change as soon as the diffraction lines become diffuse, the a axis is shrinking more continuously. For $La[Fe(CN)_6]_{3/4}\cdot xH_2O$, from the (002) and (102) diffraction lines, we estimate a reduction of a, c and V on heating from 70 to 100 °C of 1, 6 and 8%, and from 70 to 270 °C of 8, 8 and 22%.

The non-magnetic low-spin state of Fe^{II} and Ru^{II} was confirmed by magnetic measurements between 4 and 300 K. The temperature-independent susceptibility was found to be $\chi_{mol}=-4.1\times10^{-8}$ and -3.1×10^{-8} μ_B/Oe f.u. for $La[Fe(CN)_6]_{3/4}\cdot6.5H_2O$ and $La[Ru(CN)_6]_{3/4}\cdot6.5H_2O$, respectively. Using the Curie–Weiss law between 4 and 150 K without correcting the diamagnetic contributions, we derived for $Tb[Ru(CN)_6]_{3/4}\cdot6.5H_2O$ an effective moment of 9.55 μ_B and a paramagnetic Curie temperature $\Theta_p=-3$ K (the theoretical value for the free-ion moment of Tb^{3+} is 9.72 μ_B).

Although warned by discrepancies in the literature, we had not expected to meet such a complicated situation. One point that these 4:3 compounds have in common with the other rare-earth transition-element cyanides is that the lanthanum members are always easiest to crystallize and they adopt a hexagonal structure similar to the archetype $LaFe(CN)_6\cdot5H_2O$.

Acknowledgments

F.H. and H.V. thank Michael Leopold and Stefan Siegrist for experimental help and Professor H.C. Siegmann as well as the Swiss National Science Foundation for continuous support.

References

1 W.E. Bailey, R.J. Williams and W.O. Milligan, *Acta Crystallogr., Sect. B, 29* (1973) 1365.
2 G.W. Beall, D.F. Mullica and W.O. Milligan, *Acta Crystallogr., Sect. B, 34* (1978) 1446.
3 D.F. Mullica, W.O. Milligan and J.D. Oliver, *Inorg. Nucl. Chem. Lett., 15* (1979) 1.
4 D.F. Mullica, E.L. Sappenfield and H.O. Perkins, *J. Solid State Chem., 73* (1988) 65.
5 W.O. Milligan, D.F. Mullica and H.O. Perkins, *Inorg. Chim. Acta, 60* (1982) 35.
6 X.-L. Xu and F. Hulliger, *Eur. J. Solid State Inorg. Chem., 27* (1990) 443.
7 W. Petter, V. Gramlich and F. Hulliger, *J. Solid State Chem., 82* (1989) 161.
8 D.F. Mullica and E.L. Sappenfield, *J. Solid State Chem., 82* (1989) 168.
9 W. Petter, V. Gramlich, F. Hulliger and H. Vetsch, *Eur. J. Solid State Inorg. Chem., 29* (1992) 65.
10 V.G. Kuznetsov, Z.V. Popova and G.B. Seifer, *Russ. J. Inorg. Chem., 15* (1970) 1071.
11 V.G. Kuznetsov and R.T. Yakovleva, *Russ. J. Inorg. Chem., 20* (1975) 1013.
12 F. Králik, J. Meindl, Z. Tauer and D. Maletič, *Coll. Czech. Chem. Commun., 38* (1973) 1466.
13 G. Brauer, *Handbuch der präparativen anorganischen Chemie*, Ferdinand Enke, Stuttgart 1981, p. 1655.
14 F. Králik, *Coll. Czech. Chem. Commun., 34* (1969) 1327; 35 (1970) 1916.
15 J. Patton and W. Reeder, *Anal. Chem., 28* (1956) 1026.
16 R.D. Shannon, *Acta Crystallogr., Sect. A, 32* (1976) 751.
17 V. Gramlich, *Acta Crystallogr., Sect. C*, to be published.